THE JOURNAL OF BIOLOGICAL CHEMISTRY VOL. 287, NO. 46, pp. 39061–39069, November 9, 2012

Identification of the Cysteine Residue Responsible for Disulfide Linkage of Na^+ Channel α and β2 Subunits*[S]

Received for publication, July 6, 2012, and in revised form, September 13, 2012 Published, JBC Papers in Press, September 19, 2012, DOI 10.1074/jbc.M112.397646

Chunling Chen[‡], Jeffrey D. Calhoun[‡1,2], Yanqing Zhang[§1], Luis Lopez-Santiago[‡], Ningna Zhou[‡], Tigwa H. Davis[‡3], James L. Salzer[§], and Lori L. Isom[‡4]

From the [‡]Department of Pharmacology and Cellular and Molecular Biology Program, University of Michigan Medical School, Ann Arbor, Michigan 48109 and the [§]Departments of Cell Biology and Neurology and the New York University Neuroscience Institute, New York University School of Medicine, New York, New York 10016

Background: Voltage-gated Na^+ channels are composed of α and β subunits.
Results: We identified the cysteine residue in β2 responsible for disulfide linkage to α.
Conclusion: α and β2 associate through a single disulfide bridge to achieve proper subcellular targeting in neurons.
Significance: Understanding how Na^+ channel complexes are formed in neurons is crucial for understanding the development of excitability.

Voltage-gated Na^+ channels in the brain are composed of a single pore-forming α subunit, one non-covalently linked β subunit (β1 or β3), and one disulfide-linked β subunit (β2 or β4). The final step in Na^+ channel biosynthesis in central neurons is concomitant α-β2 disulfide linkage and insertion into the plasma membrane. Consistent with this, *Scn2b* (encoding β2) null mice have reduced Na^+ channel cell surface expression in neurons, and action potential conduction is compromised. Here we generated a series of mutant β2 cDNA constructs to investigate the cysteine residue(s) responsible for α-β2 subunit covalent linkage. We demonstrate that a single cysteine-to-alanine substitution at extracellular residue Cys-26, located within the immunoglobulin (Ig) domain, abolishes the covalent linkage between α and β2 subunits. Loss of α-β2 covalent complex formation disrupts the targeting of β2 to nodes of Ranvier in a myelinating co-culture system and to the axon initial segment in primary hippocampal neurons, suggesting that linkage with α is required for normal β2 subcellular localization *in vivo*. WT β2 subunits are resistant to live cell Triton X-100 detergent extraction from the hippocampal axon initial segment, whereas mutant β2 subunits, which cannot form disulfide bonds with α, are removed by detergent. Taken together, our results demonstrate that α-β2 covalent association via a single, extracellular disulfide bond is required for β2 targeting to specialized neuronal subcellular domains and for β2 association with the neuronal cytoskeleton within those domains.

Voltage-gated Na^+ channels are heterotrimeric complexes containing a single pore-forming α subunit, a non-covalently linked β1 or β3 subunit, and a covalently linked β2 or β4 subunit (1). Although Na^+ channel β subunits are non-pore-forming, they play essential roles in channel targeting and regulation of channel gating and voltage dependence, and they play channel-independent roles in cell adhesion (2). Na^+ channel β2 subunits (encoded by *Scn2b*) are disulfide-linked to the ion-conducting α subunit and are expressed in brain, peripheral nerve, and heart (3–5). Similar to the other Na^+ channel β subunit family members, β2 is a type 1 transmembrane protein containing an extracellular N-terminal V-set Ig domain, a single transmembrane segment, and an intracellular C-terminal domain. In *Xenopus* oocytes, β2 modulates $Na_v1.2$ channel gating and increases functional channel expression through promotion of intracellular vesicle fusion with the plasma membrane as measured by changes in cell capacitance (3). In transfected fibroblasts, β2 increases $Na_v1.2$ cell surface expression only if β1 is also expressed (6). β2 functions as a *trans* homophilic cell adhesion molecule *in vitro*, resulting in recruitment of ankyrin to points of cell-cell contact (7). The extracellular β2 Ig domain associates with the extracellular domain of β1 in an *in vitro* cell adhesion assay, suggesting that these two subunits may associate via cell-adhesive interactions *in vivo* (8). Similar to the other Na^+ channel β subunits, β2 can be detected in detergent-resistant membrane preparations from primary neurons and is sequentially cleaved by β and γ secretases (9). The cleaved intracellular domain of β2 is postulated to translocate to the nucleus to modulate *Scn1a* α subunit gene transcription (10); however, the regulation of this process is not understood. A series of studies has demonstrated that β2 plays important roles *in vivo* in both neurons and cardiac myocytes. *Scn2b* null mice have significantly reduced (~50–60%) tetrodotoxin-sensitive Na^+ current density in brain and small dorsal root ganglion (DRG)[5] neurons, altered voltage dependence of Na^+ current inactivation, reduced sensitivity to pain, and increased suscep-

* This work was supported, in whole or in part, by National Institutes of Health Grants NS076752 and NS 064245 (to L. L. I.) and NS043474 (to J. L. S.). This work was also supported by National Multiple Sclerosis Society Grants RG 4748A13 (to J. L. S.) and RG 3771A4/3 (to L. L. I.).
[S] This article contains supplemental Table 1.
[1] Both authors contributed equally to this work.
[2] Supported by a fellowship from the American Epilepsy Society.
[3] Present address: Dept. of Biology, Georgetown University, Washington, D. C. 20057-1229.
[4] To whom correspondence should be addressed: Dept. of Pharmacology, University of Michigan Medical School, 3422 Med Sci I, SPC 5632, 1301 Catherine St., Ann Arbor, MI 48109-5632. E-mail: lisom@umich.edu.

[5] The abbreviations used are: DRG, dorsal root ganglion; AIS, axon initial segment.

tibility to seizures (5, 11). *Scn2b* has been implicated in disease; *Scn2b* expression is up-regulated in a neuropathic pain model (12), and *Scn2b* null mice have a neuroprotective phenotype in a model of demyelinating disease (13). The *Scn2b* null mutation has been proposed to prevent pathologic Na^+ channel up-regulation along axons in response to demyelination, thus attenuating the extent of neuronal degeneration. Although *SCN2B* has not yet been linked to human brain disease, mutations in *SCN2B* are associated with atrial fibrillation in the heart (14).

Concomitant covalent linkage of α to β2 through disulfide bonding and insertion into the plasma membrane are the final steps in Na^+ channel biosynthesis in primary neurons (15). These results suggested that covalent linkage of α to β2 may occur at the extracellular face of the plasma membrane; however, the specific cysteine residue(s) involved have not been identified. Here we show, using a mutagenesis study, that a single cysteine-to-alanine substitution at the β2 extracellular residue Cys-26 is sufficient to disrupt the formation of α-β2 covalent complexes *in vitro*. Although β2WT subunits do not affect the level of Na^+ current expressed by $Na_v1.1$ in a heterologous system, co-expression of $Na_v1.1$ with β2C26A results in decreased Na^+ current compared with α alone, suggesting that β2C26A may cause intracellular retention of a population of α subunits. Using a primary myelinating co-culture system, we demonstrate that, whereas β2WT traffics to nodes of Ranvier and heminodes, β2C26A is targeted to the axonal compartment but is not detectable at nodes or heminodes. In cultured hippocampal neurons, β2WT is enriched in the AIS, as defined by anti-ankyrin G staining, whereas β2C26A is expressed in a non-polarized distribution in all of the neuronal processes. Thus, covalent linkage of β2 to α is essential for proper targeting of this subunit to specialized subcellular neuronal compartments. Finally, β2WT subunits are resistant to live cell detergent extraction from the hippocampal AIS, whereas mutant β2 subunits, which cannot form disulfide bonds with α, are removed by detergent. Taken together, our results demonstrate that α-β2 covalent association via a single, extracellular disulfide bond is required for β2 targeting to specialized neuronal subcellular domains and for β2 association with the neuronal cytoskeleton within those domains.

EXPERIMENTAL PROCEDURES

Antibodies—For immunoprecipitation and Western blot studies, primary antibodies used included rabbit polyclonal anti-pan-VGSC antibody obtained from Sigma (S6936; 1:200 dilution) and mouse monoclonal anti-V5 antibody obtained from AbD Serotec (MCA1360; 1:300 dilution). For immunofluorescence studies, primary antibodies used included rabbit antibody against ankyrin G (S. Lux, Yale University School of Medicine (New Haven, CT); 1:4,000 dilution), goat antibody against GFP (AbD Serotec; 1:4,000 dilution), guinea pig antibody against Caspr/Neurexin IV (1:4,000 dilution; M. Bhat, University of Texas (San Antonio, TX)), and chicken antibodies against MBP (Chemicon (Temecula, CA); 1:100 dilution) and MAP2 (Covance; 1:10,000 dilution). Secondary donkey antibodies conjugated to Rhodamine Red-X, Alexa Fluor 488, aminomethylcoumarin acetate, or DyLight 649 were obtained from Jackson ImmunoResearch Laboratories (West Grove, PA) and used at 1:200 dilution.

Plasmids and Cell Culture—To generate a C-terminal β2V5 epitope-tagged expression plasmid, cDNA encoding rat β2 (minus the termination codon) was cloned into the multiple cloning site of pcDNA3.1/V5-His (+) using standard TA cloning. This plasmid is referred to here as β2V5. Mutagenesis of β2 cysteine residues to alanine within this vector was performed using the QuikChange II site-directed mutagenesis kit (Stratagene). A subset of β2 constructs, including β2WT, Φ (the construct with all cysteine residues mutated to alanine), and β2C26A, were subcloned into pEGFP-N1 to add a C-terminal GFP epitope tag. The integrity of all plasmids was confirmed by DNA sequencing at the University of Michigan DNA Sequencing Core. HEK-293 cells stably expressing human $Na_v1.1$ (GenBank™ accession number NP_008851.3; HEKh$Na_v1.1$) were obtained from GlaxoSmithKline under a materials transfer agreement as described previously (16).

Co-immunoprecipitation—Co-immunoprecipitation was performed similarly as described in Ref. 17. Briefly, HEKh-$Na_v1.1$ cells cultured as described (16) were transfected with 4 μg of β2WT or mutant plasmid using Fugene 6 as recommended by the manufacturer. Protein A-Sepharose beads (Sigma) were washed with PBS and resuspended in 500 μl of dilution buffer (DB) (60 mM Tris/HCl, pH 7.5, 180 mM NaCl, 1.25% Triton X-100, 6 mM EDTA, pH 8, containing Complete Mini protease inhibitor tablets (Roche Applied Science) at 2 times the manufacturer's recommended concentration) at 4 °C. The beads were then incubated overnight at 4 °C with 5 μg of anti-pan-Na^+ channel antibody. The transfected cells were detached from the culture dishes using 50 mM Tris, 10 mM EGTA (pH 8) and centrifuged at 5,000 rpm in a microcentrifuge for 5 min at 4 °C. The cell pellet was resuspended in DB for cell lysis. After 30 min of lysis on ice, a 10-min centrifugation at 10,000 rpm in a microcentrifuge was performed to remove insoluble material. The resulting supernatant was added to the beads and incubated by rotating end-over-end for 5 h at 4 °C. The beads were then washed twice with washing buffer (50 mM Tris, pH 7.5, 150 mM NaCl, 0.1% Triton X-100, 0.02% SDS, 5 mM EDTA, pH 8, containing Complete Mini protease inhibitor tablets at 2 times the manufacturer's recommended concentration) followed by one wash with the same buffer lacking Triton X-100. Samples were then separated by SDS-PAGE on a 5% polyacrylamide gel and transferred to nitrocellulose for Western blot analysis. Western blotting was performed using the SnapId system (Millipore). Immunoblots were probed with anti-V5 or anti-pan-VGSC antibody as indicated, detected with Westfemto Chemiluminescent reagent (Pierce), and imaged using autoradiography film (Denville Scientific) or using the LI-COR Odyssey® Fc imaging system. All results presented are representative of at least two independent repeats, as specified in the figure legends.

Surface Biotinylation—Surface biotinylation of β2WT or mutant proteins was performed as described previously (16). Briefly, membrane proteins were biotinylated using the Cell Surface Labeling Accessory Pack (Pierce) following the manufacturer's instructions utilizing Complete Mini (Roche Applied Science) as protease inhibitor. Samples were separated on 12%

SDS-polyacrylamide gels. Proteins were transferred to nitrocellulose membranes that were processed for Western blotting using the SnapId system (Millipore). Anti-V5 immunoreactive signals detecting β2 subunits were compared with the immunoreactive signal for Na^+/K^+ ATPase β1 subunit, a loading control for cell surface protein preparations (16). All results presented are representative of at least two independent repeats, as specified in the figure legends.

Immunocytochemical Analysis of β2 Expression in HEK Cells—HEKhNa$_v$1.1 cells were transiently transfected with GFP alone, β2WT-GFP, β2C26A-GFP, or Φ-GFP using Fugene 6 following the manufacturer's recommendations. 24 h post-transfection, cells were replated onto 8-well glass chamber slides (BD Falcon). 24 h later, cells were fixed for 20 min at room temperature with 4% paraformaldehyde. After a 1-h blocking step (PBSTGS; dPBS containing 10% goat serum and 0.3% Triton X-100), cells were incubated overnight at room temperature with rabbit anti-GFP antibody (Invitrogen; A6455; 1:1000) diluted in PBSTGS. Following three 10-min washes with dPBS, cells were incubated for 2 h at room temperature with Alexa Fluor 568 goat anti-rabbit secondary antibody (Invitrogen; A-11011; 1:500) diluted in PBSTGS. After three 10-min washes with dPBS, slides were allowed to dry for 20 min and coverslipped using mounting medium (Invitrogen; ProLong Gold Antifade Reagent with DAPI; P36931). Slides were imaged using a Nikon A1R confocal microscope utilizing Nikon NIS-Elements software located in the Department of Pharmacology at the University of Michigan.

Whole-cell Patch Clamp Recording and Analysis—HEKhNa$_v$1.1 cells were transfected with V5- or GFP-tagged β2 subunits as described above and plated for electrophysiological analysis. To detect cells that were transfected with V5-tagged plasmids, a 1:10 ratio of GFP/β2 cDNA was used such that β2-expressing cells could be detected by epifluorescence. Aliquots of each transfection were analyzed for protein expression by Western blot to confirm protein expression. Micropipettes were obtained from capillary glass tubing (Warner Instruments) using a horizontal P-97 puller (Sutter Instruments). Micropipette resistance was between 1.5 and 3.5 megaohms when filled with intracellular solution containing 10 mM NaCl, 10 mM CsCl, 105 mM (cesium) aspartate, 10 mM EGTA, and 10 mM HEPES, pH 7.4, with CsOH and extracellular solution containing 130 mM NaCl, 4 mM KCl, 1.5 mM $CaCl_2$, 1 mM $MgCl_2$, 5 mM glucose, 10 mM HEPES, pH 7.4, with NaOH. Voltage pulses were applied, and data were recorded using Clampex version 9.2 or 10, an Axopatch 200B or 700B amplifier, and a Digidata 1322A digitizer (Molecular Devices). Pipette and whole cell capacitance were fully compensated. When appropriated, series resistance compensation was set to ~40–70% with the lag set to 10 μs. Signals were low pass-filtered at 5 kHz, and data were sampled at 40 kHz online. To determine the Na^+ current amplitude and voltage dependence of activation, Na^+ currents were evoked by 250 ms depolarizing test pulses (from −110 to 40 mV at 5 and 10 mV intervals) from a holding potential of −80 mV and a hyperpolarizing −120 mV, 250 ms prepulse. Peak Na^+ current was normalized to cell capacitance and used to plot *I*-V curves and also to calculate conductance ($g = I/(V - V_{rev})$, where V is the test potential, and V_{rev} is the measured reversal potential). Voltage dependence of inactivation was determined by applying a 50 ms test pulse to 0 mV after 250 ms prepulses to the same voltages as described for the voltage dependence of activation. Peak currents were normalized to the maximum peak I_{Na} amplitude. Normalized activation and inactivation curves were fit with a Boltzmann equation, $1/(1 + \exp(V - V_{½})/\kappa)$, where $V_{½}$ is the membrane potential in the midpoint of the curve, and κ as the slope factor. The kinetics of inactivation were measured during the test pulse to 0 mV from the same protocol used for voltage dependence of activation. The current, from 90% of the peak amplitude to 20 ms after the test pulse was initiated, was fitted to a double exponential equation of the form, $I = (F_f \times \exp(-\tau/\tau_f)) + (Fs \times \exp(-\tau/\tau_s) + C$, using the Chebyshev method, where I is the current, τ_f and τ_s are the time constants for the fast and slow inactivation component, and C is the persistent current. Analysis of the recorded Na^+ current was performed using the software packages Clampfit version 10 (Molecular Devices) and SigmaPlot version 11.2 (Systat Software, Inc., San Jose, CA). The statistical significance of differences between mean values for β2C26A-GFP or Φ-GFP compared with β2WT-GFP was evaluated using Student's unpaired *t* test, with $p < 0.05$ considered significant. Results are presented as means ± S.E.

Myelinating Co-cultures—Co-cultures of rat Schwann cells and DRG neurons were established as described previously (18). Briefly, DRGs were removed from Glu-15 or Glu-16 rat spinal cords, dissociated with 0.25% trypsin, and plated onto Matrigel (BD Biosciences)-coated coverslips. After cycling with antimitotics to eliminate non-neuronal cells, Schwann cells were added to the cultures and maintained in C medium (containing 10% fetal bovine serum, 50 ng/ml 2.5S nerve growth factor, 0.4% glucose, and 2 mM L-glutamine in minimum essential medium) for 1–3 days before adding 50 μg/ml ascorbic acid to allow myelination to ensue.

Primary Hippocampal Neuron Cultures—Primary cultures of hippocampal neurons were established essentially as described previously (19). Briefly, hippocampi from embryonic day 18 rats were treated with 0.05% trypsin (Invitrogen) in dissecting solution (0.6% glucose, 10 mM HEPES in PBS) for 30 min at 37 °C, and cells were dissociated by repeated passage through a fire-polished constricted Pasteur pipette and then plated onto 12-mm coverslips coated with poly-L-lysine (0.1 mg/ml in PBS) in minimal essential medium containing Earle's salts and glutamine with 10% FBS, 0.45% glucose, 1 mM pyruvate, and penicillin and streptomycin. After 2 h, the medium was replaced by Neurobasal medium (Invitrogen) with 2% B-27, and 0.5 mM L-glutamine. Cultures were maintained at 37 °C in a humidified 5% CO_2 atmosphere until used.

Nucleofection—Nucleofector™ technology was used to introduce β2-GFP constructs into DRG neurons prior to co-culture with Schwann cells or into hippocampal neurons. Nucleofection was performed with the Amaxa Rat Neuron Nucleofector Kit (Lonza) by using Nucleofector II (Lonza).

Immunofluorescence and Imaging—Hippocampal neurons or myelinating co-cultures were fixed in 4% paraformaldehyde for 10 min, permeabilized, and blocked with buffer containing 1% donkey serum, 5% BSA, and 0.2% Triton X-100 in 1× PBS for 30 min and then stained with primary and secondary anti-

A.

```
            21   26        98
hβ2      LPCTFNSC... GIYNCYI
hβ4      LPCTFSSC... GKYTCHV
hβ1      ILC--ISC... GDYECHV
```

B.

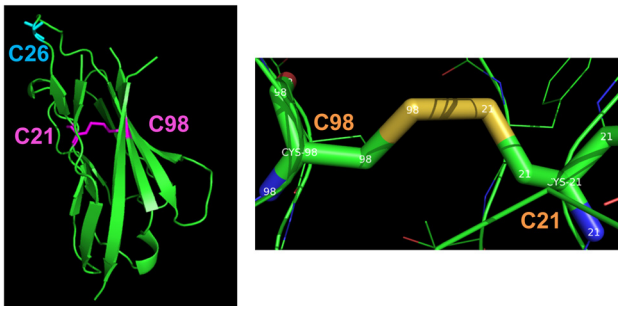

FIGURE 1. **Structural predictions for β2.** *A*, alignment of the N-terminal regions of human β2, β4, and β1 with conserved cysteine residues highlighted in *boldface type*. Residue numbering corresponds to β2. *B*, *left*, the crystal structure of the Ig loop of human myelin P_0 (30) was used as a template to show the predicted position of β2Cys-26 (*cyan*), β2C21 (*magenta*), and β2C98 (*magenta*). *Right*, the crystal structure of the Ig loop of human myelin P_0 (30) was used as a template to show the predicted intramolecular disulfide bond between β2Cys-21 and β2Cys-98.

bodies diluted in blocking buffer. Immunofluorescence images of cultures were taken with a Zeiss LSM 510 Meta confocal microscope.

Triton Extraction—Live hippocampal cultures were incubated in extraction buffer (30 mM PIPES, 1 mM $MgCl_2$, 5 mM EDTA, 0.5% Triton X-100) for 20 min at 37 °C and then rinsed in PBS, fixed in 4% paraformaldehyde, and processed for immunofluorescence.

Protein Structure Modeling—The extracellular domain of β2 was modeled based on the reported crystal structure for rat myelin P_0ex (20) using PyMOL (version 1.5.0.4; Schrödinger, LLC, New York).

Multiple Alignments of Na$^+$ *Channel Sequences*—Multiple alignments of Na^+ channel polypeptide sequences were performed using MEGA version 5 (21) utilizing the ClustalW methodology (22). NCBI GenBank™ accession numbers used in the alignment are provided in supplemental Table 1.

RESULTS

Na^+ channel β2 subunits contain five extracellular cysteine residues (Cys-21, Cys-26, Cys-43, Cys-46, and Cys-98) and one intracellular cysteine residue (Cys-143) (3). Two of the extracellular cysteine residues form an intramolecular disulfide bridge as part of the Ig-fold structure (3). Aligning the amino acid sequence of β2 with β1 and β4, we found that β2Cys-21 and β2Cys-98 were conserved among the three β subunits, suggesting that these residues are responsible for formation of the Ig loop intramolecular disulfide bridge that is common to all three (Fig. 1*A*). β3 was not included in this alignment because evidence suggests that it does not participate in homophilic cell-cell adhesion and thus may have a slightly different Ig domain structure (23). β2Cys-98 aligns with β1Cys-121, which is proposed to be critical to formation of the disulfide bridge in the Ig loop domain. β1Cys-121 is mutated to tryptophan in human epilepsy, resulting in disruption of β1-mediated cell-cell adhesion (24). These data support the idea that β2Cys-21 and β2Cys-98 participate in intramolecular disulfide bond formation in the Ig domain. Comparing β2 with β4 (25), the β subunits that are disulfide-linked to α, we found that β2Cys-26 is conserved between subunits, whereas β2Cys-43 and β2Cys-46 are not conserved, suggesting that Cys-26 may be involved in disulfide linkage to α. In previous studies, we used the crystal structure of the myelin P_0 extracellular domain to model the Na^+ channel β1 Ig loop (26). Employing a similar strategy here for the related β2 extracellular domain, we show that β2Cys-21 and β2Cys-98 are optimally aligned to form an intramolecular disulfide bond (Fig. 1*B*, *left* and *right*). In contrast, β2Cys-26 is located in the linker region between the B and C faces of the Ig loop (26), in a position that is more accessible for association with Na^+ channel α subunits (Fig. 1*B*, *left*). Thus, we hypothesized that β2Cys-26 was the most logical candidate to form an intermolecular disulfide bridge between β2 and α.

β2Cys-26 Mediates the Disulfide Linkage between β2 and α—To identify the β2 cysteine residue(s) responsible for α-β2 linkage, β2 mutant expression constructs were generated, substituting each single cysteine to alanine. In addition, every possible combination of multiple cysteine to alanine substitutions was generated, in the event that multiple cysteine residues were involved in α-β2 linkage. Each construct was engineered to contain a C-terminal V5 epitope tag to facilitate biochemical identification. β2WT or cysteine-to-alanine β2 mutant constructs were then expressed separately in HEKhNa$_v$1.1 cells. Na$_v$1.1 was immunoprecipitated with anti-pan-Na^+ channel antibody, and α-β2 protein complexes (M_r > 250,000) were detected by non-reducing SDS-PAGE followed by immunoblotting with a mouse monoclonal anti-V5 antibody to label V5-tagged β2 subunits. As expected (15), co-expression of β2WT with Na$_v$1.1 resulted in detection of a high M_r α-β2 channel complex (Fig. 2, *A* and *B*). Mutation of all six cysteine residues within β2 (Φ) completely disrupted α-β2 association (Fig. 2*A*). A single alanine substitution, C26A, was sufficient to disrupt the α-β2 linkage (Fig. 2*A*). Of all of the possible β2 cysteine-to-alanine mutant constructs, only those with the β2C26A mutation abolished β2-Na$_v$1.1 association under non-reducing conditions (Fig. 2*B* and Table 1). Importantly, mutation of β2Cys-21 or β2Cys-98, the residues proposed to form the intramolecular Ig loop disulfide bond, to alanine did not disrupt intermolecular α-β2 subunit association. All of the cysteine-to-alanine mutant β2 constructs displayed robust expression levels in cell lysates collected post-transfection (β2WT, Φ, and β2C26A shown in Fig. 2*C*; others not shown). These data suggest that a single extracellular cysteine residue, β2Cys-26, mediates the disulfide linkage between β2 and α.

Cell Surface Expression and Modulation of Na$^+$ *Currents*—The β2 mutant polypeptides Φ and β2C26A do not form disulfide bonds with Na$_v$1.1. Nevertheless, these subunits traffic to the cell surface, where they may be available to modulate Na^+ currents through non-covalent association with α. Surface biotinylation analyses, shown in Fig. 3, *A* and *B*, demonstrated that β2WT, Φ, and β2C26A are expressed at the cell surface. Fluorescence immunocytochemical data (Fig. 3*C*) confirmed cell surface expression of all three subunits. To test for the pos-

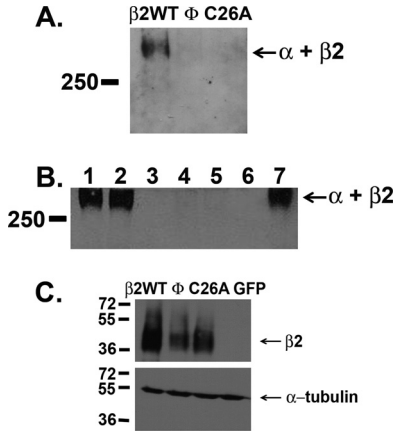

FIGURE 2. **Na$^+$ channel β2 and α subunits are disulfide-linked at β2 residue Cys-26.** Coimmunoprecipitation was performed with HEKhNa$_v$1.1 cells transiently transfected with V5-tagged β2WT or various β2 cysteine-to-alanine mutants, as indicated. Solubilized Na$_v$1.1 complexes were immunoprecipitated with anti-pan-Na$^+$ channel antibody and separated on non-reducing SDS-polyacrylamide gels as described under "Experimental Procedures." Western blots were detected with anti-V5 antibody to visualize high α-β2 protein complexes (*arrows*). *A*, disulfide-linked α-β2WT complexes are detected, whereas α-ϕ and α-β2C26A are not detectable, indicating that disulfide linkage between subunits was lost. *B*, α-β2WT (*lane 1*), α-β2C43A (*lane 2*), and α-β2C43A/C46A/C143A (*lane 7*) complexes are detected. In contrast, α-β2C26A/C43A (*lane 4*) and α-β2C26A/C43A/C46A/C143A (*lane 5*) complexes are not detectable, indicating that disulfide linkage between subunits was lost. *Lanes 3* and *6* were left empty. Results of similar experiments for the remaining β2 constructs are summarized in Table 1. *C*, Western blot analysis shows robust expression of β2WT and mutant constructs. *Top*, HEKhNa$_v$1.1 cells were transfected with V5-tagged β2WT, Φ, or β2C26A or with GFP alone, as indicated. Cells were then solubilized and analyzed by Western blot with anti-V5 antibody to confirm subunit expression. *Bottom*, the blot was stripped and reprobed with anti-α-tubulin as a loading control. Results presented in this figure are representative of five independent experiments.

TABLE 1

Detection of β2-Na$_v$1.1 disulfide linkage by coimmunoprecipitation

Coimmunoprecipitation was performed with HEKhNa$_v$1.1 cells transiently transfected with V5-tagged β2WT or various β2 cysteine-to-alanine mutants, as indicated. Solubilized Na$_v$1.1 complexes were immunoprecipitated with anti-pan-Na$^+$ channel antibody and separated on non-reducing SDS-polyacrylamide gels as described under "Experimental Procedures." Western blots were detected with anti-V5 antibody to visualize high α-β2 protein complexes, as demonstrated in Fig. 2. Results presented in this table are representative of two independent experiments, except for β2WT ϕ, β2C26A, β2C43A, β2C43A/C46A/C143A, β2C26A/C43A, and β2C26A/C43A/C46A/C143A, which were performed five times each.

Construct	Detection of immunoreactive Na$_v$1.1-β2 protein complex by SDS-PAGE
β2WT	Yes
Φ	No
β2C21A	Yes
β2C26A	No
β2C43A	Yes
β2C46A	Yes
β2C98A	Yes
β2C143A	Yes
β2C26A/C43A	No
β2C43A/C46A/C143A	Yes
β2C26A/C43A/C46A/C143A	No
β2C26A/C43A/C46A/C98A/C143A	No
β2C21A/C43A/C46A/C98A/C143A	Yes
β2C21A/C26A/C46A/C98A/C143A	No
β2C21A/C26A/C43A/C46A/C143A	No

sibility of non-covalent association of these mutant subunits with α, we co-immunoprecipitated HEKhNa$_v$1.1 cells transfected with Φ or β2C26A with anti-pan-Na$^+$ channel antibody (as in Fig. 2) and probed the Western blot for non-disulfide-linked β2 subunits (migrating in the 33 kDa range) but were unable to detect any bands (not shown). Despite these results, we could not rule out the possibility that non-disulfide-linked β2 subunits, especially β2C26A, in which the Ig loop domain is predicted to remain intact, may associate transiently with α subunits. To test this possibility, we investigated the effects of β2WT, β2C26A, or Φ on Na$^+$ currents in transfected HEKhNa$_v$1.1 cells under whole cell voltage clamp (Table 2). The V5- and GFP-tagged plasmids for each construct yielded similar results, and thus values were pooled. Similar to previous work with other Na$^+$ channel α subunits co-expressed with β2 in heterologous cells (6, 14), we observed that co-expression of β2WT with Na$_v$1.1 did not change the level of Na$^+$ current density compared with that observed for α alone. Co-expression of Φ with Na$_v$1.1 also had no effect on Na$^+$ current density compared with α alone (Fig. 4). In contrast, we observed that co-expression of β2C26A with Na$_v$1.1 resulted in a significant decrease in transient Na$^+$ current compared with WT (Fig. 4). Interestingly, these data are analogous to results reported for the *SCN2B* atrial fibrillation mutations R28Q and R28W, located in a similar region of the β2 Ig domain, which decreased the amplitude of Na$_v$1.5-expressed currents compared with β2WT (14). Also similar to (14) and to our results with Na$_v$1.5 expressed in a heterologous system (4), β2WT did not increase Na$_v$1.5-generated currents compared with α alone (14). In addition to the effect of β2C26A on current density, we observed a small but significant depolarizing shift in the voltage dependence of Na$^+$ current inactivation in the presence of Φ compared with α alone. Thus, although we were unable to detect non-covalent association of β2C26A or Φ with Na$_v$1.1 biochemically, our electrophysiological results suggest that these subunits may associate with α through low affinity interactions.

Disulfide Linkage of β2 with α Is Critical for β2 Targeting to Nodes of Ranvier and the AIS—Na$^+$ channel clustering at nodes of Ranvier is critical for action potential conduction in myelinated axons. Localization of β2 to nodes of Ranvier (28) suggests a functional role for this non-pore-forming subunit in these highly organized structures. Na$^+$ channel α subunits traffic normally to nodes of Ranvier in *Scn2b* null mice, demonstrating that β2 is not necessary for proper nodal localization and clustering of the ion channel pore. However, action potential conduction is significantly decreased in *Scn2b* null optic nerve, indicating that the density of Na$^+$ channel α subunits at the node is reduced compared with WT.

To test whether α-β2 subunit disulfide linkage affects β2 targeting to nodes, we generated myelinating co-cultures consisting of DRG neurons and Schwann cells. Prior to co-culture, neurons were transfected with β2WT-GFP, β2C26A-GFP, or Φ-GFP. C-terminal GFP epitope tags were added to the constructs to facilitate imaging of β2 localization. We examined the targeting of these constructs to heminodes (*i.e.* the initial nodal clusters that form at the ends of individual myelin segments) and to mature nodes, which are flanked on both sides by myelin segments. β2WT-GFP was targeted specifically to nodes of Ranvier as well as to the heminodes (Fig. 5*A*, *top panels*). Thus, all nodes (20 of 20) and all heminodes (44 of 44) scored in a representative experiment were labeled by the β2WT-GFP construct. These results also indicate that the C-terminal GFP tag does not interfere with normal β2 trafficking in neurons. In

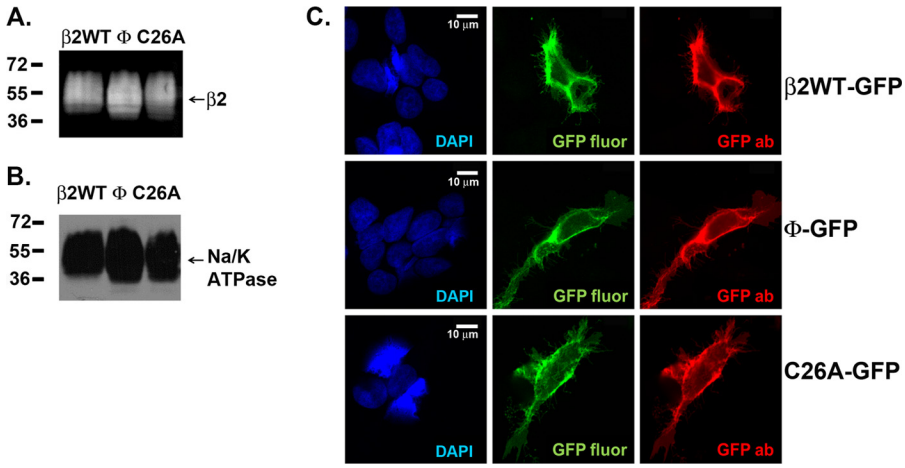

FIGURE 3. ***β*2WT, Φ, and *β*2C26A subunits are expressed at the cell surface.** *A*, cell surface biotinylation was performed on HEKhNa$_v$1.1 cells transfected with *β*2WT, Φ, or *β*2C26A as described under "Experimental Procedures." Immunoreactive bands were detected with anti-V5 antibody. The position of *β*2 subunit migration on the gel is indicated by the *arrow*. Similar to previous experiments to assess *β*1 subunit cell surface expression using this method (27), we observed multiple V5 immunoreactive bands, probably representing various levels of avidin attachment to *β*2. *B*, Na/K ATPase *β*1 subunit immunoreactivity of samples from *A* as a loading control for cell surface proteins (*arrows*). *C*, HEKhNa$_v$1.1 cells expressing *β*2WT-GFP (*top*), Φ-GFP (*center*), or *β*2C26A-GFP (*bottom*) were processed for immunocytochemistry as described under "Experimental Procedures." Cells were visualized for GFP epifluorescence (*green*) or with an anti-GFP antibody (*red*; Alexa Fluor 568) by confocal microscopy. DAPI (*blue*) indicates cell nuclei. *Scale bar*, 10 *μ*m. Results presented in this figure are representative of five independent experiments.

TABLE 2
Modulation of Na$^+$ current properties by *β*2 subunits

	GFP	*β*2WT	Φ	*β*2C26A
I_{Na} peak (pA/picofarads)	−147.7 ± 30.7	−149.8 ± 20.7	−144.3 ± 35.1	−95.8 ± 11.5[a]
I_{Na} persistent (pA/picofarads)	−14.0 ± 5.9	−24.1 ± 8.2	−9.8 ± 2.7	−7.8 ± 1.9
τ_{inac} fast (ms)	0.78 ± 0.16	0.74 ± 0.12	0.62 ± 0.05	0.62 ± 0.03
τ_{inac} slow (ms)	5.55 ± 1.2	6.17 ± 0.77	4.81 ± 0.79	4.25 ± 0.45
n	10	13	9	12
V_{rev} (mV)	67.2 ± 5.6	68.6 ± 4.5	73.8 ± 7.4	59.7 ± 6.3
n	7	10	8	10
Voltage dependence of activation				
G_{max} (nS)	35.5 ± 5.9	32.0 ± 4.0	31.7 ± 13.9	31.5 ± 7.5
K	4.6 ± 0.7	5.0 ± 0.6	5.0 ± 0.9	5.1 ± 0.5
$V_{½}$ (mV)	−19.6 ± 1.6	−19.4 ± 1.3	−14.8 ± 2.4	−19.4 ± 2.2
Voltage dependence of inactivation				
K	−5.2 ± 0.3	−6.7 ± 0.6	−5.0 ± 0.2	−5.2 ± 0.3
$V_{½}$ (mV)	−44.1 ± 2.7	−44.4 ± 2.1	−38.9 ± 1.0[β]	−44.6 ± 2.2
C	0.04 ± 0.01	0.06 ± 0.01	0.05 ± 0.01	0.06 ± 0.01

[a] $p = 0.036$ compared with WT.
[b] $p = 0.044$ compared with WT.

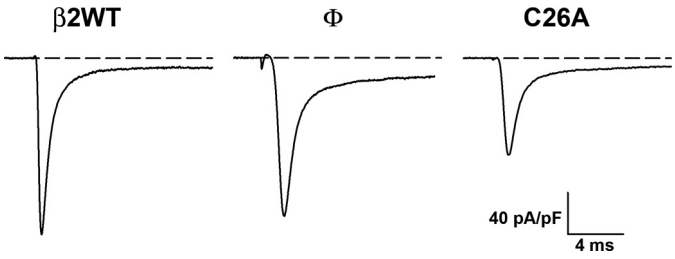

FIGURE 4. **Representative Na$^+$ current traces.** Representative Na$^+$ currents evoked by a depolarizing pulse to 0 mV were obtained from HEKhNa$_v$1.1 cells transfected with *β*2WT-GFP, Φ-GFP, or *β*2C26A-GFP, as indicated.

contrast to *β*2WT-GFP, Φ-GFP (Fig. 5*A*, *middle panels*) and *β*2C26A-GFP (Fig. 5*A*, *bottom panels*) were diffusely expressed in the neurites of the sensory neurons but absent from the nodes and heminodes. In the case of Φ-GFP, 0 of 52 heminodes and 0 of 21 nodes were positive; *β*2C26A-GFP was present in 0 of 48 heminodes and 0 of 12 nodes. Thus, although *β*2 subunits that are not covalently linked to *α* still traffic to the neurites, they fail to cluster at nodes or heminodes.

Na$^+$ channel clustering at the AIS is critical for action potential initiation. We tested the targeting of *β*2WT-GFP, Φ-GFP, and *β*2C26A-GFP to the AIS using primary hippocampal neuronal cultures. Similar to our results in myelinating co-cultures, we found that disruption of *α*-*β*2 covalent linkage disrupted *β*2 targeting. *β*2WT-GFP was enriched at the AIS, defined by ankyrin-G expression, in 59 of 60 neurons scored. (It was exclusively expressed in the AIS in 5 of 60 neurons and faintly expressed in the remainder of the axon in 22 of 60 neurons and in all processes in 32 of 60 neurons) (Fig. 5*B*, *top panels*). In contrast, the Φ-GFP (Fig. 5*B*, *middle panels*) and *β*2C26A-GFP (Fig. 5*B*, *bottom panels*) constructs failed to concentrate at the AIS in any neurons scored (*i.e.* 0 of 54 and 60 neurons, respectively). Rather, expression of both constructs was either nonpolarized or confined to the dendrites. Finally, we used the live cell detergent extraction technique (18) to investigate the association of *β*2 subunits with cytoskeletal elements at the AIS. As shown in Fig. 5*C*, *β*2WT subunits are resistant to Triton X-100 extraction from the hippocampal AIS (Fig. 5*C*, *top panels*). In contract Φ-GFP (Fig. 5*C*, *middle panels*) and *β*2C26A-GFP

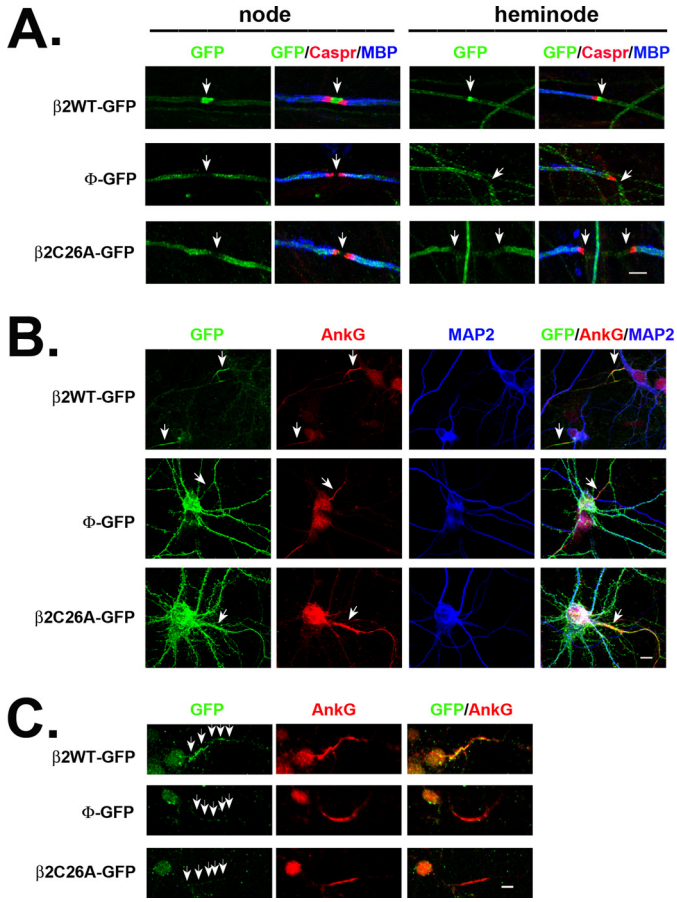

FIGURE 5. **Covalent α-β2 linkage is critical for targeting of β2 to nodes of Ranvier and the AIS.** *A*, targeting of β2 constructs to nodes of Ranvier. DRG neurons were nucleofected with WT or mutant β2-GFP constructs, as indicted, and then co-cultured with Schwann cells under myelinating conditions for ~2 weeks. Cultures were fixed and analyzed by immunofluorescence staining. β2WT-GFP (*green*) accumulated at nodes and heminodes (*arrows*), whereas the mutant constructs failed to accumulate at these sites. Paranodes were stained with Caspr (*red*), and myelin segments were stained with MBP (*blue*). *Scale bar*, 5 μm. *B*, targeting of β2 constructs in hippocampal neurons. β2-GFP constructs were nucleofected into hippocampal neurons and analyzed at 18 days *in vitro*. β2WT-GFP (*green*) was enriched in the AIS, labeled by ankyrin G staining (*red*) (*arrows*). In contrast, Φ-GFP and β2C26A-GFP mutants (*green*) were equally distributed in axons and dendrites or preferentially concentrated in dendrites and were not enriched in the AIS. Dendrites were stained with MAP2 (*blue*). *Scale bar*, 10 μm. *C*, Triton X-100 extracts mutant β2 constructs from hippocampal neuron cultures. β2WT-GFP nucleofected hippocampal neuron cultures were extracted with Triton X-100 prior to fixation and then fixed and stained. The β2WT-GFP construct was retained at the AIS despite detergent treatment and was extracted from other sites. Both Φ-GFP and β2C26A-GFP were largely extracted from the neurons, including from the AIS, by detergent treatment. *Arrows* in the GFP staining panels delineate the positions of AIS; neuronal somata are located on the *left*. *Scale bar*, 5 μm.

(Fig. 5*C*, *bottom panels*), subunits that cannot form disulfide bonds with α are removed completely by detergent treatment. Taken together, these results demonstrate that α-β2 covalent association is required for β2 targeting to specialized neuronal subcellular domains and for β2 association with the neuronal cytoskeleton within those domains.

DISCUSSION

Voltage-gated Na^+ channels are essential regulators of neuronal excitability in mammals (1). Concomitant covalent association of Na^+ channel α with β2 subunits and insertion into the plasma membrane are the final steps in channel biosynthesis in central neurons (15). Thus, α-β2 association is considered to be a critical rate-limiting step in the formation of functional Na^+ channels and consequently the development of excitability, playing an essential role in the regulation of channel density and channel targeting to specialized locations in the neuron (15). Studies with *Scn2b* null mice have demonstrated that β2 subunits are critical regulators of central and peripheral neuronal excitability *in vivo* via modulation of channel cell surface expression (5, 11). Here we set out to close a critical gap in the Na^+ channel literature: the molecular identification of the site of covalent α-β2 association.

Via a combination of molecular biological, biochemical, and electrophysiological techniques, we show that the β2 residue Cys-26 is necessary and sufficient to mediate α-β2 covalent association through disulfide bonding. We also expressed these constructs in primary hippocampal neurons and in myelinating co-cultures to investigate the role of covalent α subunit association in β2 targeting to the AIS and nodes of Ranvier, respectively. Mutation of β2 extracellular residue Cys-26 to alanine resulted in disruption of α-β2 covalent association. Despite the disruption of covalent α-β2 association by this amino acid substitution, co-expression of β2C26A with $Na_v1.1$ decreased the level of transient Na^+ current density compared with expression of α alone, suggesting that β2C26A and α may associate through transient, non-covalent interactions that we were unable to detect using biochemical techniques. The β2WT subunit is enriched in the AIS of hippocampal neurons and selectively expressed at nodes and heminodes in myelinating DRG-Schwann cell co-cultures. In contrast, β2C26A was not enriched in the AIS of hippocampal neurons but rather was diffusely expressed in both axons and dendrites or just in dendrites, indicating that its targeting was dramatically altered. Similarly, in myelinating co-cultures, β2C26A was never expressed at nodes but rather remained diffusely distributed along the neurites. Triton X-100 extraction of hippocampal neurons removed β2C26A from the AIS but left β2WT undisturbed, suggesting that β2 subunits are normally associated with the neuronal cytoskeleton and that disruption of α-β2 covalent association eliminates β2 cytoskeletal interactions. These data suggest that α-β2 subunit covalent association is essential for proper β2 clustering at specialized neuronal subcellular domains. In other words, β2 follows α. Further, β2 interactions with the cytoskeleton at the AIS may be mediated exclusively through Na^+ channel α subunits rather than through other cell adhesion molecules or via direct association with cytoskeletal proteins. We demonstrated previously, using a heterologous system, that β2 binds to the cytoskeletal protein ankyrin in response to cellular aggregation (7). Based on these results, we predict that β2-β2 *trans* homophilic adhesion (*e.g.* through axonal fasciculation) may be required to transduce an outside-in signal to stimulate β2 association with ankyrin in neurons. In the absence of β2-β2 *trans* adhesion, as is the case in the neuronal cultures used here, β2 does not associate with other β2 subunits on adjacent cells and thus does not bind ankyrin. In this case, β2 must depend on covalent linkage with α for the cytoskeletal association.

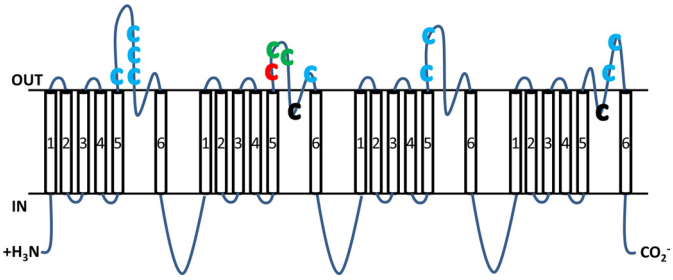

FIGURE 6. **Map of conserved extracellular Cys residues within Na$^+$ channel α subunits.** Locations of cysteine residues within the topology of the α subunit are denoted by *C*. All extracellular cysteine residues map to S5-S6 loop regions. 12 candidate residues are extracellular, whereas two residues are embedded in the membrane as part of a P loop region and are indicated in *black*. The *color* of the *letter C* denotes the amount of evolutionary conservation. Conservation in all sequences tested is denoted by *blue*; conservation in mammalian and *E. electricus* Na_v is denoted by *green*; and conservation in mammalian channels only is denoted by *red*.

Previous work proposed that the A/A′ face of the extracellular β1 Ig loop domain is critical for $Na_v1.2$ modulation (26). In addition, the extracellular segment IVSS2-S6 of $Na_v1.2$ was shown to play a dominant role in α-β1 subunit association (29). These critical regions of β1 association may be conserved in multiple Na$^+$ channel α subunits. Our results here, identifying β2Cys-26 as the critical residue responsible for covalent α-β2 linkage, raise the question of which cysteine residue on the α subunit forms the corresponding disulfide bridge with β2. Although experiments to address this question are beyond the scope of the current study, we took an *in silico* approach to identify potential extracellular α subunit cysteine residues based on evolutionary conservation. Analysis of a multiple alignment of a set of Na$^+$ channel α subunit amino acid sequences, including mammalian (human, mouse, and rat) $Na_v1.1$, $Na_v1.2$, $Na_v1.6$, and $Na_v1.7$, identified a set of 12 conserved, candidate cysteine residues within the extracellular portions of domain I–IV S5-S6 loops (Fig. 6). Further analysis of a multiple alignment containing the same mammalian protein sequences as well as two additional non-mammalian Na$^+$ channel coding sequences (*Electrophorus electricus* Na_v and *Drosophila* paralytic) demonstrated that nine of the 12 cysteine residues are conserved in all of the sequences. Interestingly, three of the cysteine residues within the domain II S5-S6 loop are less conserved. Two of these residues are conserved in *Electrophorus electricus* Na_v but not in the *Drosophila paralytic*, whereas a single cysteine residue was conserved only in mammalian channels and not in *E. electricus* Na_v or in *D. paralytic*. Given that neither *Drosophila* nor *E. electricus* contain genes orthologous to the mammalian Na$^+$ channel β subunits, these three, less conserved, cysteine residues are attractive candidates for the formation of a disulfide bond with β2Cys-26 in mammals. Although the *in silico* analysis suggests a subset of three candidate cysteine residues, it is impossible to determine the exact cysteine residue(s) involved based on evolutionary conservation alone. Future mutagenesis studies will allow for the elucidation of the exact cysteine residue on α subunits that fulfills this role.

REFERENCES

1. Catterall, W. A. (2012) Voltage-Gated Sodium Channels at 60. Structure, Function, and Pathophysiology. *J. Physiol.* **590,** 2577–2589
2. Brackenbury, W. J., and Isom, L. L. (2011) Na Channel β Subunits. Overachievers of the Ion Channel Family. *Front. Pharmacol.* **2,** 53
3. Isom, L. L., Ragsdale, D. S., De Jongh, K. S., Westenbroek, R. E., Reber, B. F., Scheuer, T., and Catterall, W. A. (1995) Structure and function of the β2 subunit of brain sodium channels, a transmembrane glycoprotein with a CAM motif. *Cell* **83,** 433–442
4. Dhar Malhotra, J., Chen, C., Rivolta, I., Abriel, H., Malhotra, R., Mattei, L. N., Brosius, F. C., Kass, R. S., and Isom, L. L. (2001) Characterization of sodium channel α- and β-subunits in rat and mouse cardiac myocytes. *Circulation* **103,** 1303–1310
5. Lopez-Santiago, L. F., Pertin, M., Morisod, X., Chen, C., Hong, S., Wiley, J., Decosterd, I., and Isom, L. L. (2006) Sodium channel β2 subunits regulate tetrodotoxin-sensitive sodium channels in small dorsal root ganglion neurons and modulate the response to pain. *J. Neurosci.* **26,** 7984–7994
6. Kazarinova-Noyes, K., Malhotra, J. D., McEwen, D. P., Mattei, L. N., Berglund, E. O., Ranscht, B., Levinson, S. R., Schachner, M., Shrager, P., Isom, L. L., and Xiao, Z. C. (2001) Contactin associates with Na$^+$ channels and increases their functional expression. *J. Neurosci.* **21,** 7517–7525
7. Malhotra, J. D., Kazen-Gillespie, K., Hortsch, M., and Isom, L. L. (2000) Sodium channel β subunits mediate homophilic cell adhesion and recruit ankyrin to points of cell-cell contact. *J. Biol. Chem.* **275,** 11383–11388
8. McEwen, D. P., and Isom, L. L. (2004) Heterophilic interactions of sodium channel β1 subunits with axonal and glial cell adhesion molecules. *J. Biol. Chem.* **279,** 52744–52752
9. Wong, H. K., Sakurai, T., Oyama, F., Kaneko, K., Wada, K., Miyazaki, H., Kurosawa, M., De Strooper, B., Saftig, P., and Nukina, N. (2005) β subunits of voltage-gated sodium channels are novel substrates of BACE1 and γ-secretase. *J. Biol. Chem.* **280,** 23009–23017
10. Kim, D. Y., Carey, B. W., Wang, H., Ingano, L. A., Binshtok, A. M., Wertz, M. H., Pettingell, W. H., He, P., Lee, V. M., Woolf, C. J., and Kovacs, D. M. (2007) BACE1 regulates voltage-gated sodium channels and neuronal activity. *Nat. Cell Biol.* **9,** 755–764
11. Chen, C., Bharucha, V., Chen, Y., Westenbroek, R. E., Brown, A., Malhotra, J. D., Jones, D., Avery, C., Gillespie, P. J., 3rd, Kazen-Gillespie, K. A., Kazarinova-Noyes, K., Shrager, P., Saunders, T. L., Macdonald, R. L., Ransom, B. R., Scheuer, T., Catterall, W. A., and Isom, L. L. (2002) Reduced sodium channel density, altered voltage dependence of inactivation, and increased susceptibility to seizures in mice lacking sodium channel β2-subunits. *Proc. Natl. Acad. Sci. U.S.A.* **99,** 17072–17077
12. Pertin, M., Ji, R. R., Berta, T., Powell, A. J., Karchewski, L., Tate, S. N., Isom, L. L., Woolf, C. J., Gilliard, N., Spahn, D. R., and Decosterd, I. (2005) Up-regulation of the voltage-gated sodium channel β2 subunit in neuropathic pain models. Characterization of expression in injured and non-injured primary sensory neurons. *J. Neurosci.* **25,** 10970–10980
13. O'Malley, H. A., Shreiner, A. B., Chen, G. H., Huffnagle, G. B., and Isom, L. L. (2009) Loss of Na$^+$ channel β2 subunits is neuroprotective in a mouse model of multiple sclerosis. *Mol. Cell Neurosci.* **40,** 143–155
14. Watanabe, H., Darbar, D., Kaiser, D. W., Jiramongkolchai, K., Chopra, S., Donahue, B. S., Kannankeril, P. J., and Roden, D. M. (2009) Mutations in sodium channel β1- and β2-subunits associated with atrial fibrillation. *Circ. Arrhythm. Electrophysiol.* **2,** 268–275
15. Schmidt, J. W., and Catterall, W. A. (1986) Biosynthesis and processing of the alpha subunit of the voltage-sensitive sodium channel in rat brain neurons. *Cell* **46,** 437–444
16. Patino, G. A., Brackenbury, W. J., Bao, Y., Lopez-Santiago, L. F., O'Malley, H. A., Chen, C., Calhoun, J. D., Lafrenière, R. G., Cossette, P., Rouleau, G. A., and Isom, L. L. (2011) Voltage-gated Na$^+$ channel β1B. A secreted cell adhesion molecule involved in human epilepsy. *J. Neurosci.* **31,** 14577–14591
17. Rusconi, R., Scalmani, P., Cassulini, R. R., Giunti, G., Gambardella, A., Franceschetti, S., Annesi, G., Wanke, E., and Mantegazza, M. (2007) Modulatory proteins can rescue a trafficking-defective epileptogenic Nav1.1 Na$^+$ channel mutant. *J. Neurosci.* **27,** 11037–11046
18. Zhang, Y., Bekku, Y., Dzhashiashvili, Y., Armenti, S., Meng, X., Sasaki, Y., Milbrandt, J., and Salzer, J. L. (2012) Assembly and maintenance of nodes of Ranvier rely on distinct sources of proteins and targeting mechanisms. *Neuron* **73,** 92–107
19. Dzhashiashvili, Y., Zhang, Y., Galinska, J., Lam, I., Grumet, M., and Salzer,

J. L. (2007) Nodes of Ranvier and axon initial segments are ankyrin G-dependent domains that assemble by distinct mechanisms. *J. Cell Biol.* **177,** 857–870
20. Shapiro, L., Doyle, J. P., Hensley, P., Colman, D. R., and Hendrickson, W. A. (1996) Crystal structure of the extracellular domain from P_0, the major structural protein of peripheral nerve myelin. *Neuron* **17,** 435–449
21. Tamura, K., Peterson, D., Peterson, N., Stecher, G., Nei, M., and Kumar, S. (2011) MEGA5. Molecular evolutionary genetics analysis using maximum likelihood, evolutionary distance, and maximum parsimony methods. *Mol. Biol. Evol.* **28,** 2731–2739
22. Thompson, J. D., Higgins, D. G., and Gibson, T. J. (1994) ClustalW. Improving the sensitivity of progressive multiple sequence alignment through sequence weighting, position-specific gap penalties, and weight matrix choice. *Nucleic Acids Res.* **22,** 4673–4680
23. McEwen, D. P., Chen, C., Meadows, L. S., Lopez-Santiago, L., and Isom, L. L. (2009) The voltage-gated Na^+ channel β3 subunit does not mediate *trans* homophilic cell adhesion or associate with the cell adhesion molecule contactin. *Neurosci. Lett.* **462,** 272–275
24. Meadows, L. S., Malhotra, J., Loukas, A., Thyagarajan, V., Kazen-Gillespie, K. A., Koopman, M. C., Kriegler, S., Isom, L. L., and Ragsdale, D. S. (2002) Functional and biochemical analysis of a sodium channel β1 subunit mutation responsible for generalized epilepsy with febrile seizures plus type 1. *J. Neurosci.* **22,** 10699–10709
25. Yu, F. H., Westenbroek, R. E., Silos-Santiago, I., McCormick, K. A., Lawson, D., Ge, P., Ferriera, H., Lilly, J., DiStefano, P. S., Catterall, W. A., Scheuer, T., and Curtis, R. (2003) Sodium channel β4, a new disulfide-linked auxiliary subunit with similarity to β2. *J. Neurosci.* **23,** 7577–7585
26. McCormick, K. A., Isom, L. L., Ragsdale, D., Smith, D., Scheuer, T., and Catterall, W. A. (1998) Molecular determinants of Na^+ channel function in the extracellular domain of the β1 subunit. *J. Biol. Chem.* **273,** 3954–3962
27. Patino, G. A., Claes, L. R., Lopez-Santiago, L. F., Slat, E. A., Dondeti, R. S., Chen, C., O'Malley, H. A., Gray, C. B., Miyazaki, H., Nukina, N., Oyama, F., De Jonghe, P., and Isom, L. L. (2009) A functional null mutation of SCN1B in a patient with Dravet syndrome. *J. Neurosci.* **29,** 10764–10778
28. Kaplan, M. R., Cho, M. H., Ullian, E. M., Isom, L. L., Levinson, S. R., and Barres, B. A. (2001) Differential control of clustering of the sodium channels $Na_v1.2$ and $Na_v1.6$ at developing CNS nodes of Ranvier. *Neuron* **30,** 105–119
29. Qu, Y., Rogers, J. C., Chen, S. F., McCormick, K. A., Scheuer, T., and Catterall, W. A. (1999) Functional roles of the extracellular segments of the sodium channel α subunit in voltage-dependent gating and modulation by β1 subunits. *J. Biol. Chem.* **274,** 32647–32654
30. Liu, Z., Wang, Y., Yedidi, R. S., Brunzelle, J. S., Kovari, I. A., Sohi, J., Kamholz, J., and Kovari, L. C. (2012) Crystal structure of the extracellular domain of human myelin protein zero. *Proteins* **80,** 307–313